

Temperature-dependent vacancy formation during the growth of Cu on Cu(001)

C. E. Botez and P. F. Miceli

Department of Physics and Astronomy, University of Missouri-Columbia, Columbia, Missouri 65211

P. W. Stephens

Department of Physics, State University of New York, Stony Brook, New York 11794

(Received 26 April 2002; published 20 November 2002)

X-ray diffraction measurements show that a large number of vacancies are incorporated in thin Cu films grown on Cu(001) at low temperatures. At any given deposition temperature between 110 and 160 K, the vacancy concentration c_v , obtained from reflectivity data, does not change with the coverage Θ , for 2.5 ML $\leq \Theta \leq 20$ ML. However, c_v is *temperature dependent*: for 15-ML-thick films, grown at different temperatures, it monotonically decreases with increasing T from $c_v \approx 2\%$ at 110 K to zero at $T = 160$ K. A different “ c_v vs T ” dependence is observed for films grown at 110 K and then annealed at progressively higher temperatures. Here $c_v \approx 2\%$ persists over a broad temperature interval (between 110 and 200 K) and c_v exhibits a slower decrease upon heating, reaching zero at 300 K.

DOI: 10.1103/PhysRevB.66.195413

PACS number(s): 61.10.Kw, 68.55.Jk

INTRODUCTION

The extensive research focused on molecular beam epitaxy (MBE) is ultimately aimed at providing the ability to engineer the desired nanostructures. To accomplish this goal one needs not only to understand the microscopic kinetics of epitaxial growth, but also to control it through the tuning of certain macroscopic parameters, among which the temperature of the substrate, T , plays a central role. It is well known that T can enhance, diminish, trigger, or inhibit several microscopic mechanisms that essentially contribute to the outcome of an MBE experiment. Indeed, experimental and theoretical studies of metal homoepitaxy have shown that many quantities that describe the morphology of the evolving surface (such as the mean-square roughness σ^2 or the growth exponent β) exhibit a pronounced temperature dependence.^{1–10} Moreover, growth at different temperatures may progress in different modes, leading to qualitatively different surface morphologies, like in the case of Ag/Ag(001) epitaxy, where the surface was observed to grow via the propagation of steps (step flow) for $T > 500$ K, laterally (layer by layer) for $500 \text{ K} > T > 200$ K or vertically for $T < 200$ K.³

While it is obvious that at high enough temperatures T influences growth via the atomic surface mobility, its effects on the surface morphology at “very” low temperatures (where the adatom mobility is small) are much less understood. Recently, it was found that certain metallic surfaces, where homoepitaxy is dominated by an additional energy barrier that opposes the interlayer mass transport [Ehrlich-Schwoebel (ES) effect],¹¹ exhibit a strong temperature dependence of growth within the low- T regime. For example, He-atom scattering measurements of Cu/Cu(001) epitaxy¹² have revealed a “reentrant smooth growth” below $T = 160$ K. Similar observations were made in a recent scanning tunneling microscopy (STM) study of Ag/Ag(001) where the roughness of 25-ML-thick films was observed to decrease upon cooling between 200 and 130 K, and then increase when the growth temperature was further reduced to

50 K.⁵ This behavior, as well as other temperature-dependent effects observed during low- T homoepitaxial growth,⁷ has been explained in terms of competing uphill and downhill surface currents.^{13,14} Specific mechanisms have been proposed, such as “transient mobility,”⁷ “downward funneling,”¹⁵ or “restricted downward funneling,”⁵ and much progress has been achieved in the understanding of low- T homoepitaxial growth.^{14,16} Yet a comprehensive picture of these phenomena is not yet available largely because of the very limited number of experiments that systematically address the temperature dependence of roughening.

An important area that has received little attention is the role of subsurface defects. Molecular dynamics¹⁷ and very recent kinetic Monte Carlo simulations^{5,6} have suggested that growth at low temperatures on (001) metallic surfaces might incorporate a large concentration of vacancies in films deposited at low temperatures. Because the presence of vacancies is likely to influence the microscopic kinetic mechanisms that govern the growth on these surfaces, the process of vacancy formation could lead to very significant changes in surface morphology for low- T homoepitaxy. In a previous x-ray scattering study⁴ we reported the first experimental indication that a large compressive strain, consistent with the incorporation of an appreciable vacancy concentration ($\sim 2\%$), is present in a 15-ML-thick Cu film deposited on Cu(001) at $T = 110$ K. Recently, we obtained similar results for the low- T Ag/Ag(001) and Ag/Ag(111) epitaxy and showed that in the case of Ag(111) the vacancies have a strong effect on the surface morphology.¹⁰

Here we report x-ray scattering measurements of the temperature and coverage dependence of vacancy formation during the growth of Cu on Cu(001). We investigated Cu films with thicknesses in the range 2.5–20 ML, deposited at temperatures between 110 and 160 K. X-ray scattering is a particularly useful probe for these studies because of its unique ability to measure the surface morphology and the subsurface structure simultaneously. Previously, x rays have been used to study mismatches between the deposited film and the underlying bulk of the crystal induced by either surface

relaxation,^{18,19} incorporated defects,⁴ and surface reconstructions.²⁰ Our specular reflectivity data conclusively show that a compressive strain along the surface normal is present in the deposited films, which indicates that vacancies are incorporated through the growing surface. At a fixed temperature, the vacancy concentration c_v does not depend on the coverage. However, c_v is temperature dependent: it decreases with increasing T from $c_v \sim 2\%$ at $T=110$ K to $c_v = 0\%$ at $T=160$ K. For films deposited at 110 K and then annealed at progressively higher temperatures c_v is constant (at $\sim 2\%$) up to 200 K and subsequently decreases to zero at room temperature.

EXPERIMENTAL PROCEDURES

The x-ray scattering experiments were carried out on the SUNY X3B2 beamline at the National Synchrotron Light Source, Brookhaven National Laboratory. The Cu(001) sample was initially prepared by mechanical polishing to reduce the miscut to about 0.1° and subsequently annealed for several days in an ultrahigh-vacuum (UHV) chamber (base pressure 10^{-10} Torr) to repair the damage from polishing. Repeated cycles of Ar ion sputtering followed by 1-h annealing at 900 K, performed *in situ*, allowed us to obtain starting surfaces with large, flat terraces having a lateral size $L > 5000$ Å and a rms roughness $\sigma < 0.5$ Å. As we have demonstrated elsewhere,³ such high-quality starting surfaces are important in kinetic roughening studies in order to avoid transient effects. Before each deposition cycle, further sputtering-annealing cycles were performed on the sample and the cleanness of the surface was verified by Auger spectroscopy. No contaminants were detected at any of the temperatures used in this study. Once a smooth, clean surface was achieved, metal atoms evaporated from a thermal oven were deposited on the surface at a constant rate of ~ 1 ML/min. During the deposition, the temperature of the sample was stabilized (± 1 K) by simultaneous resistive heating and liquid-nitrogen cooling. The temperature was accurately determined by direct measurements of the lattice constant. X-ray scattering data were collected by scanning across the specular rod (transverse scans) for different values at the perpendicular momentum transfer Q_z . The specular reflectivity was obtained from the corresponding transverse profile by subtracting the diffuse scattering component.²¹

RESULTS AND DISCUSSION

Figure 1 shows the specular reflectivity data (open symbols) measured for a smooth starting Cu(001) surface at $T=160$ K (squares) and for rough surfaces, obtained by depositing 15 ML at $T=160$ K (triangles) and $T=110$ K (circles). We observe that the growth temperature has a strong effect on the reflectivity line shape. For the film grown at 160 K, the only change in the reflectivity from its ideal (perfectly truncated crystal) profile is a more accentuated dampening at Q_z —values far from the in-phase condition. This behavior is a consequence of the surface roughness that increases with the coverage and has been thoroughly analyzed in our previous studies of kinetic roughening^{3,4,22}

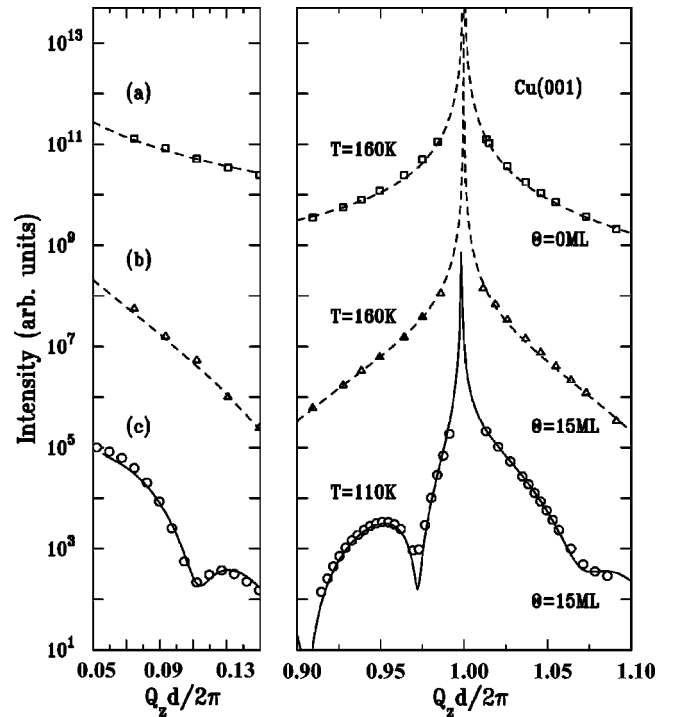


FIG. 1. Specular reflectivity from the Cu(001) surface with 0 and 15 ML deposited at $T=160$ K (squares and triangles, respectively) and with 15 ML deposited at $T=110$ K (circles). At 160 K, the only effect resulting from the growth of 15 ML on the “clean” Cu(001) substrate is that the reflectivity becomes more dampened as the surface becomes rougher—the data are well described by a simple Gaussian height fluctuation model (dashed line) that allows a precise determination of the surface mean-square roughness (Ref. 22). At 110 K, however, the reflectivity from the 15-ML-thick Cu/Cu(001) films exhibits interference fringes and a pronounced asymmetry toward higher perpendicular wave vector. Here a real-space model that includes a large compressive strain in the deposited film (solid line) is necessary to fit the data.

using a model²² that assumes height fluctuations described by Poisson statistics. The dashed lines in Fig. 1 are best fits to such a model. At 110 K, however, the reflectivity line shape exhibits two qualitatively different features: thin-film oscillations (with a periodicity that is consistent with the thickness of the Cu film) and a pronounced asymmetry about the (002) Bragg reflection. As we previously showed for Ag,¹⁰ this reflectivity profile can be very well explained by a real-space model where, in addition to roughness, a large surface-normal compressive strain is uniformly distributed throughout the deposited film. The solid line in Fig. 1, which is a best fit to such a model, matches the data excellently, yielding a 1% contraction of the film lattice constant d_{film} with respect to its bulk counterpart d_{bulk} . In regards to the origin of the strain, we emphasize that it cannot arise from an accidental low- T surface contamination for at least two reasons. First, a very large impurity concentration would be necessary in order to account its large magnitude, while Auger electron spectroscopy (AES) analysis consistently shows clean surfaces at all temperatures used in our study. Second, interstitial impurities (such as hydrogen, which is

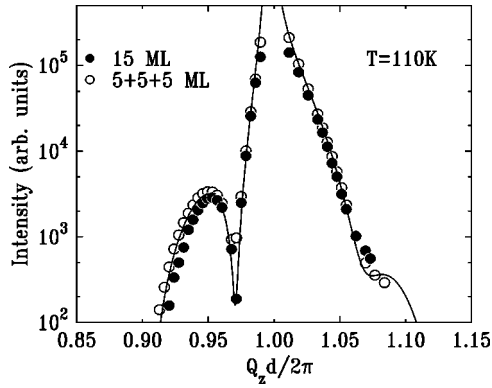


FIG. 2. Comparison between the specular reflectivity, measured around the (002) Bragg reflection, from the Cu(001) surface with 15 ML deposited at $T=110$ K in one run (solid symbols) and in three consecutive runs, 5 + 5 + 5 ML (open symbols). The two reflectivity profiles are essentially identical, demonstrating that *no* intervening impurity layers are incorporated in between the substrate and deposited film. The solid line is a best fit to a real-space model described in the text.

not detectable by AES) or impurities larger than Ag would cause a lattice expansion, instead of the observed compression. Stacking faults can also be ruled out, since they do not occur on Cu(001). In order to eliminate alternative explanations for the features observed in the low- T reflectivity line shape, we have tried several different models and found that none of these provides a satisfactory explanation of the data. For example, one might consider that the asymmetries and interference fringes present in the reflectivity profile might arise from a slightly different lattice constant of a *single* “junk layer” incorporated in between the film and substrate at the beginning of each deposition (immediately after the opening of the shutter in front of the evaporator). Such a layer would be covered with a “clean” Cu film and, therefore, not detectable by AES. To check for this possibility, we grew 15 ML of Cu on Cu(001), at $T=110$ K, in two ways: by depositing the whole amount in one run (15 ML) and cumulatively in three separate runs of 5 ML each (5 ML + 5 ML + 5 ML). If a junk layer were incorporated at the beginning of each deposition cycle, the noncumulatively deposited film would contain one junk layer, while the cumulatively deposited one would contain three equidistant junk layers. Obviously, the crystal truncation rods from these two structures would have very different profiles, but as shown in Fig. 2, the x-ray specular reflectivity [measured around the (002) Bragg reflection] from the 15 ML film (solid symbols) is essentially identical to its 5 + 5 + 5 ML counterpart (open symbols). This conclusively shows that the structures of the two films, deposited cumulatively and non-cumulatively, are the same.

We believe the strain is induced by a large vacancy concentration incorporated in the growing film because one must account for the appreciable magnitude of the strain as well as its compressive character. Moreover, vacancies are likely to be created under these far-from-equilibrium conditions, as suggested by both molecular dynamics¹⁷ and kinetic Monte Carlo simulations⁵ for metal/metal(001) homoepitaxy. An es-

timate for the vacancy concentration c_v may be obtained using the linear relationship between the isotropic strain ε and the concentration of point defects.^{23,24} This relationship has been measured²⁵ for vacancies in bulk Cu: $\varepsilon = -\alpha c_v$ where $\alpha=0.2$. There is an additional uniaxial contribution to the strain arising from the clamping of the film to the substrate. This effect is well known for strained-layer heteroepitaxial systems,²⁶ and it was observed for vacancies in Ag films on Ag(001).¹⁰ Realizing the stress-free condition of the film perpendicular to the surface, $\sigma_{zz}=0=C_{11}\varepsilon_{zz}^{\text{uni}}+C_{12}(\varepsilon_{xx}^{\text{uni}}+\varepsilon_{yy}^{\text{uni}})$ (Ref. 24) with elastic constants C_{11} and C_{12} , the condition of in-plane lattice matching between the film and substrate requires $\varepsilon_{xx}^{\text{uni}}=\varepsilon_{yy}^{\text{uni}}=-\varepsilon$. Thus the resulting strain that will be observed perpendicular to the surface is $\Delta=\varepsilon+\varepsilon_{zz}^{\text{uni}}$ so that

$$\Delta = \frac{d_{\text{film}} - d_{\text{substrate}}}{d_{\text{film}}} = -\alpha \left(1 + \frac{2C_{12}}{C_{11}} \right) c_v, \quad (1)$$

where $C_{12}/C_{11}=0.72$ for Cu. This result, which is valid for an isotropic elastic medium as well as along $\langle 001 \rangle$ for a cubically anisotropic elastic medium, assumes that the elastic constants are not significantly changed by the incorporation of vacancies. Moreover, we have assumed monovacancies for the purposes of estimation, since relaxation data are available for this case and the present experiment cannot determine whether there are single vacancies or vacancy clusters.

Figure 3 shows the specular reflectivity from Cu films of different thickness, deposited on Cu(001) at $T=110$ K, measured over an extended range of Q_z values. The three curves, which are vertically shifted for clarity, correspond to three different coverages: $\Theta=10$ ML (squares), $\Theta=15$ ML (triangles), and $\Theta=20$ ML (circles). Each of these exhibit a pronounced asymmetry about the Bragg reflection as well as thin-film interference fringes in *both* the high- and low- Q_z ranges. In a previous study of low- T Ag(001) and Ag(111) homoepitaxy¹⁰ we showed that the low-angle fringes correspond to a vertical terrace size distribution arising from a pyramidal surface morphology, whereas the high-angle fringes contain contributions from both strain and pyramids. Pyramidal surface structures occur ubiquitously in homoepitaxial growth and, specifically, they have been observed for Cu/Cu(001).^{12,27} We analyze the present data using this model, which includes an out-of-plane uniform compressive strain within the deposited film. For completeness, we mention the essential ideas of the model here, but the details can be found in Ref. 10. Since the specular reflectivity²⁸ depends on the exposed terrace area P_j , at layer height j , we introduce P_j^{pyr} for a single pyramid and take into account that there will be a statistical distribution of pyramid heights. Assuming a binomial distribution for the pyramid heights, we calculate the overall exposed terrace distribution $P_j = \langle P_j^{\text{pyr}} \rangle_{\text{all pyramids}}$. Therefore, the model includes (as parameters) an average pyramid height and height variance as well as the magnitude of the strain, with the latter being of central interest here. It is important to mention that these fit parameters are not correlated and quite independent: the strain magnitude determines the asymmetry about the Bragg reflec-

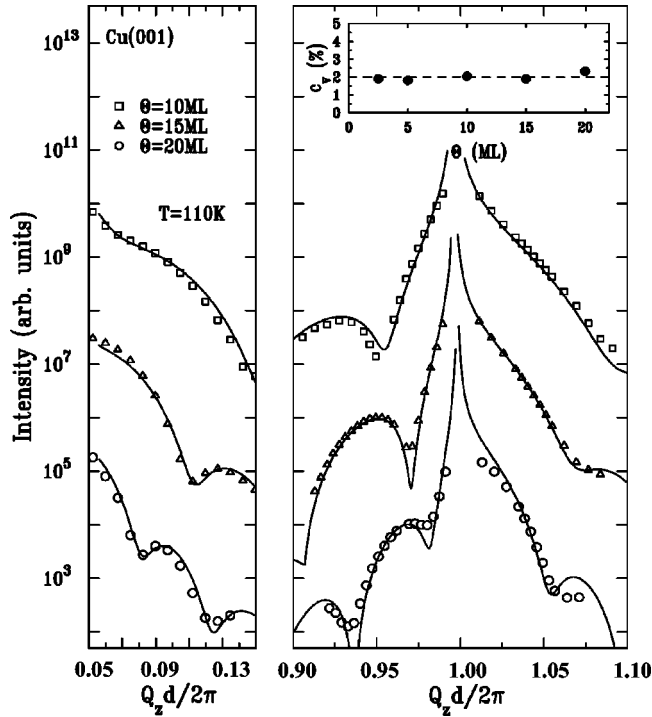


FIG. 3. Specular reflectivity measured for Cu(001) with 10 ML (squares), 15 ML (triangles), and 20 ML (circles), deposited at $T = 110$ K. The curves are vertically shifted for clarity and the solid lines represent best fits to a real-space model, described in the text. The inset shows the coverage dependence of the vacancy concentration, obtained from fits to specular reflectivity data.

tion, and the average pyramid height influences the oscillation period at low angles, while the pyramid height variance is responsible for the magnitude and decay of the oscillations.

Two important results emerge from the fits to the x-ray reflectivity data in Fig. 3. First, the magnitude of the strain turns out to be the same ($\sim 1\%$) at all coverages. Using Eq. (1), this yields the vacancy concentration shown in the inset. Thus there is a $\sim 2\%$ coverage-independent vacancy concentration in the Cu films grown on Cu(001) at $T = 110$ K. Although we cannot rule out a slight gradient in the concentration, these results indicate that the vacancies are, indeed, incorporated within the growing film. Second, there is a non-Gaussian distribution of surface heights, in contrast to the situation at higher temperatures (> 160 K). This is indicated by the appearance of thin-film interference fringes in the low- Q_z range of reflectivity, which cannot be directly explained by the vacancies or resulting strain: sufficient scattering contrast between the film and underlying bulk substrate cannot be achieved in the low- Q_z regime from the 1% contraction of the film lattice parameter or over any Q_z range from the 2% vacancy concentration. Instead, we observe that the pyramidal surface morphology, combined with the lattice contraction of the film, fits the entire range of data. The distribution of terrace heights, P_j , obtained from a fit of the model for the pyramidal surface morphology, discussed above, is shown in Fig. 4 for 10-ML- (triangles), 15-ML- (squares), and 20-ML- (circles) thick Cu films grown on

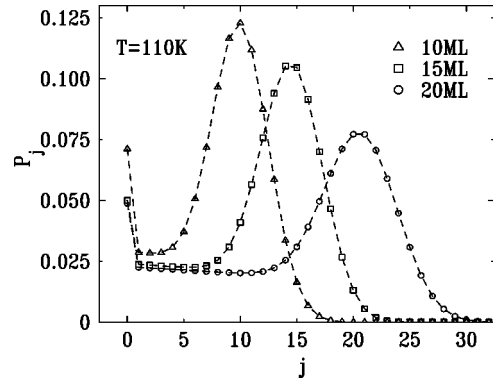


FIG. 4. Fraction of exposed surface atoms, P_j , resulting from the best fits to the Cu/Cu(001) reflectivity data in Fig. 3, as a function of the height level j for the three different coverages.

Cu(001) at 110 K. Interestingly, a non-Gaussian distribution was also observed for homoepitaxial growth on Ag(111) (Ref. 10) where there was a particularly strong pyramidal character to the P_j distribution. The case of Cu(001) appears to be intermediate between Ag(111) and Ag(001), where the latter exhibits a P_j having a Gaussian distribution to the lowest temperatures studied.¹⁰

We carried out similar measurements and analysis for Cu/Cu(001) films of different thicknesses grown at 130, 145, and 160 K. In each case the vacancy concentration c_v obtained from fits to x-ray reflectivity data is observed to be coverage independent. On the other hand, c_v strongly depends on the deposition temperature. This is demonstrated in Fig. 5, where the vacancy concentration incorporated in 15-ML-thick films is shown as a function of the deposition temperature. Here c_v monotonically decreases with increasing temperature from $T = 110$ K, where $c_v = 2.2\%$, to $T = 160$ K, where no vacancies are incorporated.

In addition to the dependence of c_v on the deposition temperature we investigated the annealing of the vacancy concentration for films deposited at a fixed low T . A 15-ML-thick Cu film was deposited at $T = 110$ K, and the tempera-

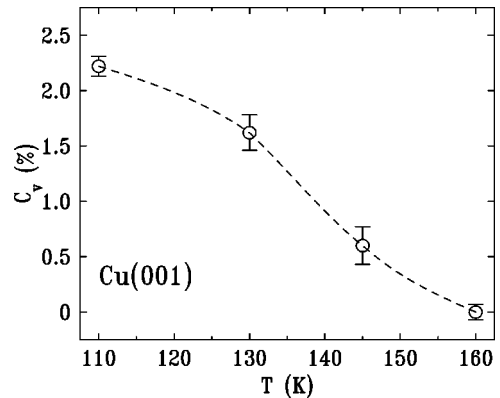


FIG. 5. Temperature dependence of the vacancy concentration c_v incorporated in 15-ML-thick Cu films deposited on Cu(001) substrates. c_v monotonically decreases with increasing growth temperature from $\sim 2\%$ at 110 K to zero at 160 K.

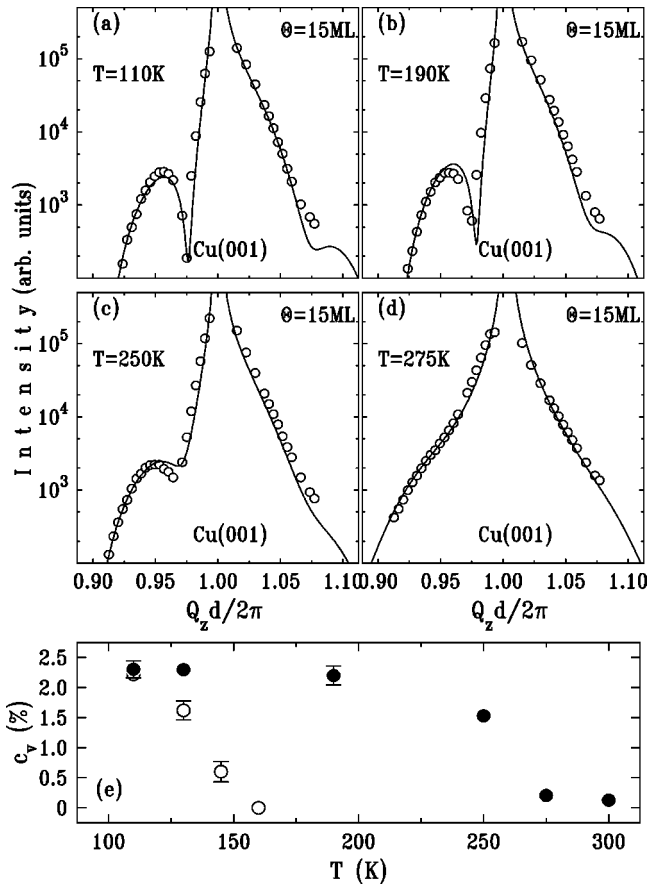


FIG. 6. (a)–(d) Temperature dependence of the reflectivity profile, measured about the (002) reflection, from a 15-ML-thick Cu film deposited on Cu(001) at $T=110\text{K}$ and then annealed at progressively higher temperatures. The solid lines are best fits allowing the determination of the vacancy concentration in the Cu films. (e) Temperature dependence of the vacancy concentration upon annealing (solid symbols) compared to the vacancy concentration incorporated in films deposited at different temperatures (open symbols).

ture was then slowly raised in $\sim 25\text{K}$ increments up to 300 K, with x-ray diffraction data collected before each temperature increase. Each step (temperature raise + x-ray measurements) took approximately 30 min. Figures 6(a)–6(d) show the reflectivity data from the 15 ML Cu/Cu(001) film measured at different temperatures during the annealing process (open circles). At $T=110\text{K}$ (the deposition temperature), the best fit [solid line in Fig. 6(a)] yields a surface-normal compressive strain of 1.1%, which corresponds to a vacancy concentration $c_v=2.3\%$. This value stays almost constant upon annealing up to $T=190\text{K}$, where our x-ray measurement and analysis [Fig. 6(b)] gives $c_v=2.2\%$. Above this temperature, however, the vacancy concentration drops significantly with increasing T and eventually vanishes at room temperature—this being evidenced in Figs. 6(c) and 6(d) by the attenuation (at 250 K) followed by the disappearance (at 275 K) of the “knee” on the low-angle side of the Bragg reflection. We found $c_v=1.5\%$ at $T=250\text{K}$ and $c_v=0.1\%$ at $T=300\text{K}$. The complete temperature behavior of the vacancy concentration upon annealing (from 110 to 300 K) is shown by the solid symbols in Fig. 6(e). We observe that it

differs from the c_v dependence on the deposition temperature (open symbols) by the fact that, once incorporated, the vacancies persist in the same concentration up to $\sim 200\text{K}$, whereas direct growth at 200 K occurs without vacancy incorporation.⁴

Our observations for the vacancy annealing [solid symbols in Fig. 6(e)] are remarkably similar to those in radiation damage studies of bulk Cu. Balluffi²⁹ reported that the vacancies anneal at $T=280\text{K}$ (our value being between 275 and 300 K), while Ehrhart *et al.*³⁰ observed a plateau in the “ c_v vs T ” dependence, between 100 and 200 K, followed by a rapid decrease of c_v that nearly vanishes at about 300 K. This behavior is in excellent agreement with our findings and represents further proof that the specular reflectivity line shape observed in our x-ray scattering experiment at low temperatures is indeed due to the incorporation of vacancies into the growing film.

Now we discuss the c_v dependence on the deposition temperature, shown by the open circles in Fig. 6(e). While, qualitatively, this is the expected behavior, it is still intriguing that the vacancy concentration decreases from an appreciable value to zero over a very narrow temperature interval, of only 50 K, indicating that the kinetic mechanisms responsible for the vacancy formation have an abrupt temperature dependence. This quick onset is also true for the recently proposed “restricted downward funneling” (RDF),^{5,6} where, instead of “funneling down” over the step edges, the depositing atoms get trapped on the sides of the larger nanoprotuberances (which become more numerous as T decreases), leading to the formation of internal voids.⁵ However, the RDF model predicts that the vacancy formation is associated with an increasingly *rougher* growth (as the deposition temperature is lowered), whereas for Cu/Cu(001) a reentrant *smooth* growth was observed within the temperature range where vacancies are incorporated by both x-ray⁴ and He-atom¹² scattering. It should be noted that there are potentially multiple (and unexplored) ways through which vacancies can affect the surface morphology. For example, a vacancy might influence the local kinetics of the atoms in its immediate vicinity, or the long-range strain field (which we observe directly in the present experiment) might also change the ES barrier. Finally, the RDF model was developed for growth on (001) surfaces, while our previous studies show that vacancies are also incorporated for the Ag/Ag(111) epitaxy^{10,31} at $T=100\text{K}$. This suggests that a more general kinetic process might be involved in vacancy formation during low- T metal homoepitaxy and further investigation is necessary to clarify this issue.

In conclusion, we have used synchrotron x-ray scattering to study the growth of Cu on Cu(001) at low temperatures. We observed that a surface-normal compressive strain is present in the Cu films deposited at temperatures below 160 K, indicating that an appreciable vacancy concentration (c_v) is present in the growing film. At a fixed temperature, c_v does not change with the thickness of the deposited film. This fact, combined with a uniformly strained film that is necessary to explain the observed x-ray reflectivity, indicates that the vacancies are incorporated within the growing film

and remain there during the subsequent growth. The vacancy concentration exhibits a well-defined temperature dependence: it monotonically decreases with increasing T from $c_v \sim 2\%$ at 110 K to $c_v = 0\%$ (no vacancies) at $T = 160$ K. We also found that the vacancies incorporated at 110 K do not anneal when the temperature of the system is raised to 200 K. Upon further heating, however, c_v slowly decreases, reaching zero at 300 K. This annealing behavior is *identical* to the annealing behavior of vacancies in bulk Cu, giving further strong evidence that the compressive strain observed in these experiments is indeed due to the incorporation of vacancies during homoepitaxial growth at low temperature. Finally, concomitant with vacancy formation, the x-ray reflectivity indicates the emergence of a surface height distri-

bution that is slightly non-Gaussian, originating from a pyramidal surface morphology.

ACKNOWLEDGMENTS

Support is acknowledged from the National Science Foundation under Contract Nos. (P.W.S.) DMR-9202528 and (P.F.M., C.E.B.) DMR-9623827 and the Midwest Superconductivity Consortium (MISCON) under DOE Grant No. DE-FG02-90ER45427. The SUNY X3 beamline is supported by the DOE, under Contract No. DE-FG02-86ER45231 and the NLSL is supported by the DOE, Division of Material Sciences and Division of Chemical Sciences. We thank Ian Robinson for the Cu crystal and for helpful discussions.

-
- ¹Z. Zhang, J. Detch, and H. Metiu, *Phys. Rev. B* **48**, 4972 (1993).
²M. C. Bartelt and J. W. Evans, *Phys. Rev. Lett.* **75**, 4250 (1995).
³W. C. Elliott, P. F. Miceli, T. Tse, and P. W. Stephens, *Phys. Rev. B* **54**, 17 938 (1996); in *Surface Diffusion: Atomistic and Collective Processes*, Vol. 360 of *NATO Advanced Study Institute, Series B: Physics*, edited by M. C. Tringides (Plenum, New York, 1997), p. 209.
⁴C. E. Botez, P. F. Miceli, and P. W. Stephens, *Phys. Rev. B* **64**, 125427 (2001).
⁵C. R. Stoldt, K. J. Caspersen, M. C. Bartelt, C. J. Jenks, and J. W. Evans, *Phys. Rev. Lett.* **85**, 800 (2000).
⁶K. J. Caspersen, C. R. Stoldt, A. R. Layson, M. C. Bartelt, P. A. Thiel, and J. W. Evans, *Phys. Rev. B* **63**, 085401 (2001).
⁷W. F. Egelhoff and I. Jacob, *Phys. Rev. Lett.* **62**, 921 (1989).
⁸D. E. Sanders and A. E. DePristo, *Surf. Sci.* **254**, 341 (1991).
⁹H.-J. Ernst, F. Fabre, and J. Lapujoulade, *Surf. Sci. Lett.* **275**, L682 (1992).
¹⁰C. E. Botez, W. C. Elliott, P. F. Miceli, and P. W. Stephens, *Phys. Rev. B* **66**, 075418 (2002).
¹¹G. Ehrlich and F. G. Hudda, *J. Chem. Phys.* **44**, 1039 (1966); R. L. Schwoebel and E. J. Shipsey, *J. Appl. Phys.* **37**, 3682 (1966).
¹²H.-J. Ernst, F. Fabre, R. Folkerts, and J. Lapujoulade, *Phys. Rev. Lett.* **72**, 112 (1994).
¹³J. Villain, *J. Phys. I* **1**, 19 (1991).
¹⁴M. C. Bartelt and J. W. Evans, *Surf. Sci.* **423**, 189 (1999).
¹⁵J. W. Evans, D. E. Sanders, P. A. Thiel, and A. E. DePristo, *Phys. Rev. B* **41**, 5410 (1990).
¹⁶J. G. Amar and F. Family, *Phys. Rev. B* **54**, 14 071 (1996).
¹⁷C. L. Kelchner and A. E. DePristo, *Surf. Sci.* **393**, 72 (1997); F. Montalenti and A. F. Voter, *Phys. Rev. B* **64**, 081401 (2001).
¹⁸C. E. Botez, W. C. Elliott, P. F. Miceli, and P. W. Stephens, *Phys. Rev. B* **63**, 113404 (2001).
¹⁹G. Helgesen, D. Gibbs, A. P. Baddorf, D. M. Zehner, and S. G. J. Mochrie, *Phys. Rev. B* **48**, 15 320 (1993).
²⁰D. Gibbs, B. M. Ocko, D. M. Zehner, and S. G. J. Mochrie, *Phys. Rev. B* **38**, 7303 (1988).
²¹I. K. Robinson and D. J. Tweet, *Rep. Prog. Phys.* **55**, 559 (1992).
²²W. C. Elliott, P. F. Miceli, T. Tse, and P. W. Stephens, *Physica B* **221**, 65 (1996).
²³J. D. Eshelby, *J. Appl. Phys.* **25**, 255 (1954).
²⁴L. D. Landau and E. M. Lifshitz, *Theory of Elasticity* (Pergamon, New York, 1970).
²⁵C. W. Tucker and J. B. Sampson, *Acta Metall.* **2**, 433 (1954); T. Broom and R. K. Ham, in *Vacancies and Other Point Defects in Metals and Alloys*, Institute of Metals Monograph and Report Series No. 23 (Institute of Metals, London, 1958), p. 41.
²⁶P. F. Miceli, K. W. Moyers, and C. J. Palmstrøm, *Appl. Phys. Lett.* **58**, 1602 (1991).
²⁷J.-K. Zuo and J. F. Wendelken, *Phys. Rev. Lett.* **78**, 2791 (1997).
²⁸P. F. Miceli, in *Semiconductor Interfaces, Microstructures and Devices: Properties and Applications*, edited by Z. C. Feng (IOP, Bristol, 1993), p. 87.
²⁹R. W. Balluffi, *J. Nucl. Mater.* **69–70**, 240 (1978).
³⁰P. Ehrhart, K. H. Robrock, and H. R. Schober, in *Physics of Radiation Effects in Crystals*, edited by R. A. Johnson and A. N. Orlov (Elsevier Science, Amsterdam, 1986), p. 60.
³¹C. E. Botez, W. C. Elliott, P. F. Miceli, and P. W. Stephens, in *Mechanisms of Surface and Microstructure Evolution in Deposited Films and Film Structures*, edited by J. G. Amar, G. H. Gilmer, M. V. R. Murthy, and J. Sanchez, Jr., *Mater. Res. Soc. Symp. Proc. No. 672* (Materials Research Society, Warrendale, 2001), p. O2.7.